Electronic Supplementary Material (ESI) for New Journal of Chemistry.
This journal is © The Royal Society of Chemistry and the Centre National de la Recherche Scientifique 2022

Supporting Information

New 3,1,2,4-benzothiaselenadiazines, related π-heterocycles including Herz cations, radicals and molecular complexes, and Bunte salts

Alexander Yu. Makarov*[,a], Yulia M. Volkova[a], Samat B. Zikirin[b], Irina G. Irtegova[a], Irina Yu. Bagryanskaya[a], Yuri V. Gatilov[a], Andrey A. Nefedov[a], Andrey V. Zibarev[a]

[a] *N. N. Vorozhtsov Institute of Organic Chemistry, Siberian Branch, Russian Academy of Sciences, 630090 Novosibirsk, Russian Federation*
Fax: +7 383 330 9752; E-mail: makarov@nioch.nsc.ru
[b] *V. V. Voevodsky Institute of Chemical Kinetics and Combustion, Siberian Branch, Russian Academy of Sciences, 630090 Novosibirsk, Russian Federation*

Contents

1. X-ray diffraction data

Table S1 Crystallographic data of compounds **3**, **24**, **25** and **25·26/27**

Compound	**3**	**24**	**25**
Empirical formula	$C_7H_6N_2OSSe$	$C_6H_4NClSSe$	$C_{14}H_{20}NS_2Cl$
Formula weight	245.16	236.57	301.88
Temperature K	296(2)	200(2)	296(2)
Wavelength Å	0.71073	0.71073	0.71073
Crystal system	Triclinic	Monoclinic	Monoclinic
Space group	P-1	$P2_1/n$	C2/m
Unit cell dimensions *a* Å	6.6599(4)	7.8867(4)	10.6876(18)
b Å	7.4329(4)	5.5755(2)	7.0309(14)

c Å	8.7949(5)	17.6217(8)	20.882(6)
α °	87.367(3)	90	90
β °	75.419(3)	97.319(2)	95.119(9)
γ °	87.060(3)	90	90
Volume $Å^3$	420.55(4)	768.55(6)	1562.9(6)
Z	2	4	4
Density (calcd.) $Mg.m^{-3}$	1.936	2.045	1.283
Abs. coefficient mm^{-1}	4.660	5.419	0.495
F(000)	240	456	640
Crystal size mm^3	0.3×0.3×0.06	0.60×0.40×0.02	0.40×0.30×0.01
Θ range for data collection °	2.4–27.5	2.3–35.0	0.98–25.0
Index ranges	$-8 \le h \le 8$, $-9 \le k \le 9$, $-11 \le l \le 11$	$-12 \le h \le 12$, $-8 \le k \le 8$, $-28 \le l \le 28$	$-12 \le h \le 12$, $-8 \le k \le 8$, $-24 \le l \le 24$
Reflections collected	7576	18803	12917
Independent reflections	1931 R(int) = 0.028	3382 R(int) = 0.064	1502 R(int) = 0.102
Completeness to θ %	99.4	99.9	99.7
Data / restraints / parameters	1931 / 0 / 110	3382 / 0 / 91	1502/ 18 / 113
Goodness-of-fit on F^2	1.10	1.02	1.08
Final R indices $I > 2\sigma(I)$	R_1 = 0.0283, wR_2 = 0.0727	R_1 = 0.0397, wR_2 = 0.0932	R_1 = 0.0931, wR_2 = 0.2361
Final R indices (all data)	R_1 = 0.0325, wR_2 = 0.0775	R_1 = 0.0521, wR_2 = 0.0994	R_1 = 0.1300, wR_2 = 0.2457
Largest diff. peak/hole $e.Å^{-3}$	0.63/–0.62	1.89/–1.20	0.70/–0.58
CCDC	**2115817**	**2115818**	**2115819**

Table S1 *(continued)*

Compound	**25·26/27**
Empirical formula	$C_{14}H_{20}NS_2Cl \cdot C_{14}H_{21.33}N_2O_2S_2Cl_{0.67}$
Formula weight	639.41
Temperature K	296(2)
Wavelength Å	0.71073
Crystal system	Triclinic
Space group	P–1
Unit cell dimensions *a* Å	10.5054(7)

b Å	12.3360(8)
c Å	14.6228(10)
α °	113.319(3)
β °	98.895(3)
γ °	103.186(3)
Volume $Å^3$	1629.55(19)
Z	2
Density (calcd.) $Mg.m^{-3}$	1.303
Abs. coefficient mm^{-1}	0.458
F(000)	677
Crystal size mm^3	0.45×0.30×0.10
Θ range for data collection °	1.4–30.7
Index ranges	$-13 \leq h \leq 13$, $-12 \leq k \leq 16$, $-18 \leq l \leq 16$
Reflections collected	10427
Independent reflections	7060 R(int) = 0.018
Completeness to θ %	99.9
Data / restraints / parameters	7060 / 2 / 371
Goodness-of-fit on F^2	1.03
Final R indices $I > 2\sigma(I)$	$R_1 = 0.0469$, $wR_2 = 0.1215$
Final R indices (all data)	$R_1 = 0.0691$, $wR_2 = 0.1370$
Largest diff. peak/hole $e.Å^{-3}$	0.600/–0.254
CCDC	**2115820**

*Salt **25** and complex **25·26/27***

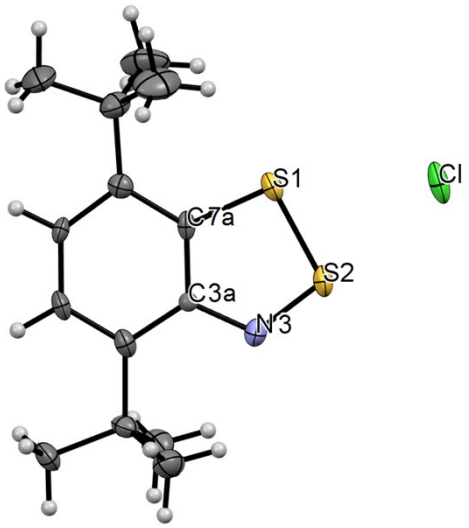

Figure S1 Individual salt **25** (CCDC 2115819), selected bond distances (Å) and angles (°): S1–S2 2.002(4), S2–N3 1.579(8), N3–C3a 1.37(1), C3a–C7a 1.43(1), C7a–S1 1.749(9); C7a–S1–S2 94.1(3), S1–S2–N3 99.1(3), S2–N3–C3a 117.7(7), N3–C3a–C7a 116.7(8), C3a–C7a–S1 112.4(7).

For salt **25**, S1…Cl^- and S2…Cl^- interionic contacts of 3.089(4) and 2.813(4) Å, respectively, are shortened as compared with the sum of corresponding van der Waals (VdW) radii of 3.55 Å.[1]

In the crystal, salt **25** reveals ion pairs featuring a single shortened contact Cl…H of 2.77 Å (the sum of VdW radii is 2.95 Å)[1] (Figure S2). Crystal complex **25·26/27** displays dimer of **26/27** molecules connected by S–O…H–N hydrogen bonds of 2.34(2) Å (the sum of VdW radii is 2.72 Å),[1] together with ion-pair dimers of **25**. The dimers of **26/27** molecules and dimers of **25** ion pairs are connected by Cl^-…H–N hydrogen bonds of 2.29(3) Å (the sum of VdW radii is 2.95 Å),[1] S…O contacts of 3.309(3) Å (the sum of VdW radii is 3.32 Å)[1] and C…O contacts of 3.060(4) and 3.041(3) Å (the sum of VdW radii is 3.22 Å)[1] forming infinite chains (Figure S3).

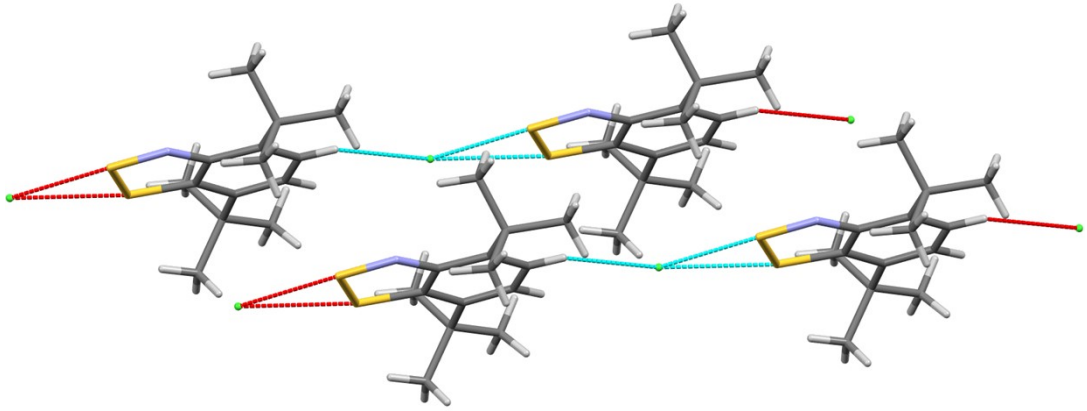

Figure S2 Shortened contacts (dashed blue and red lines) and packing fragment in crystalline **25**. Colour code: gray – C, light gray – H, green – Cl, blue – N, red – O, yellow – S.

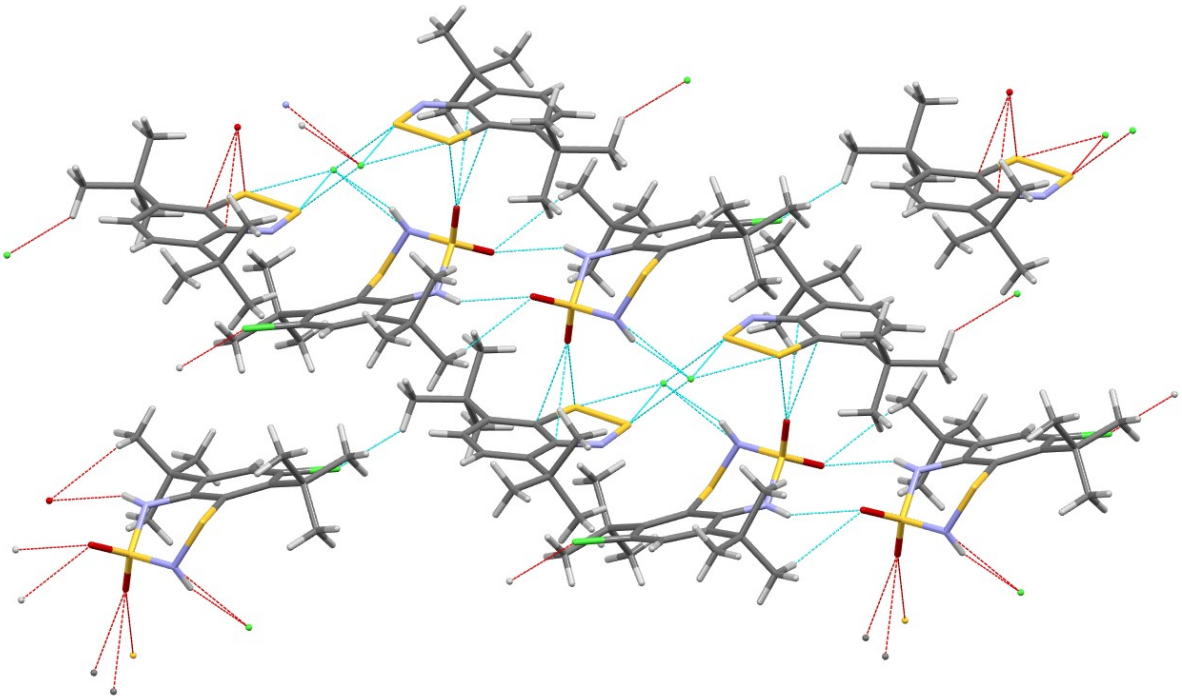

Figure S3 Shortened contacts (dashed blue and red lines) and packing fragment in crystalline complex **25**·**26**/**27**. Colour code: gray – C, light gray – H, green – Cl, blue – N, red – O, yellow – S.

2. Additional chemical experiments

Compounds **36-40** were prepared by known methods.[2] In both variants of unsuccessful cyclizations (*a* and *b*, Scheme S1) with compounds **10**, **11** and **36-39**, any heterocyclic products were not observed in the reaction mixtures; with compound **12**, ^{1}H NMR spectra revealed minor signals of compound **1**, which was not isolated due to its small abundance.

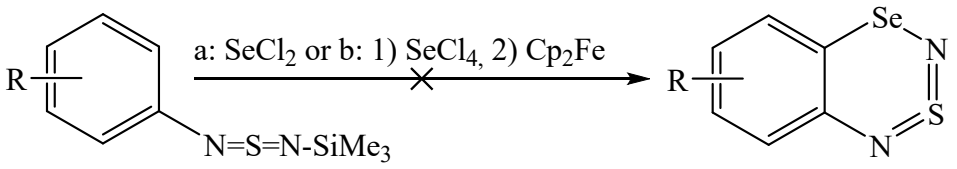

10-12, **36-39**

R = 2,4-Me_2 (**10**), 2,5-*t*-Bu_2 (**11**), 2-I (**12**), 2-OMe (**36**), 4-OMe (**37**), 2-Me (**38**), 4-Me (**39**)

Scheme S1 Unsuccessful cyclizations of compounds **10-12** and **36-39**.

Hydrolysis of 5-chloro-1,3,2,4-benzodithiadiazine **40**

Black crystals of compound **40** turned yellow after the several month-long action of air moisture. Recrystallization from hexane gave 2,2'-diamino-3,3'-dichlorodiphenyl disulfide **41** identified by ^{1}H NMR (Scheme S2).[3]

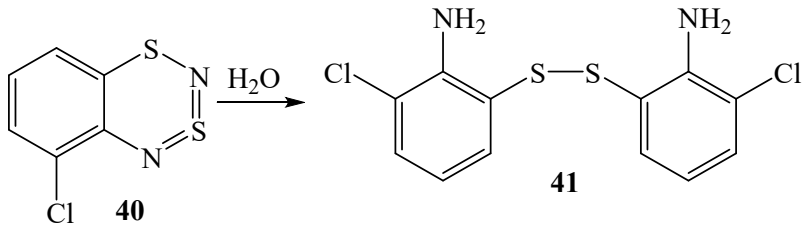

Scheme S2 Hydrolysis of dithiadiazine **40** into disulfide **41**.

3. Nuclear magnetic resonance

^{1}H NMR spectra and spin-spin coupling constants J

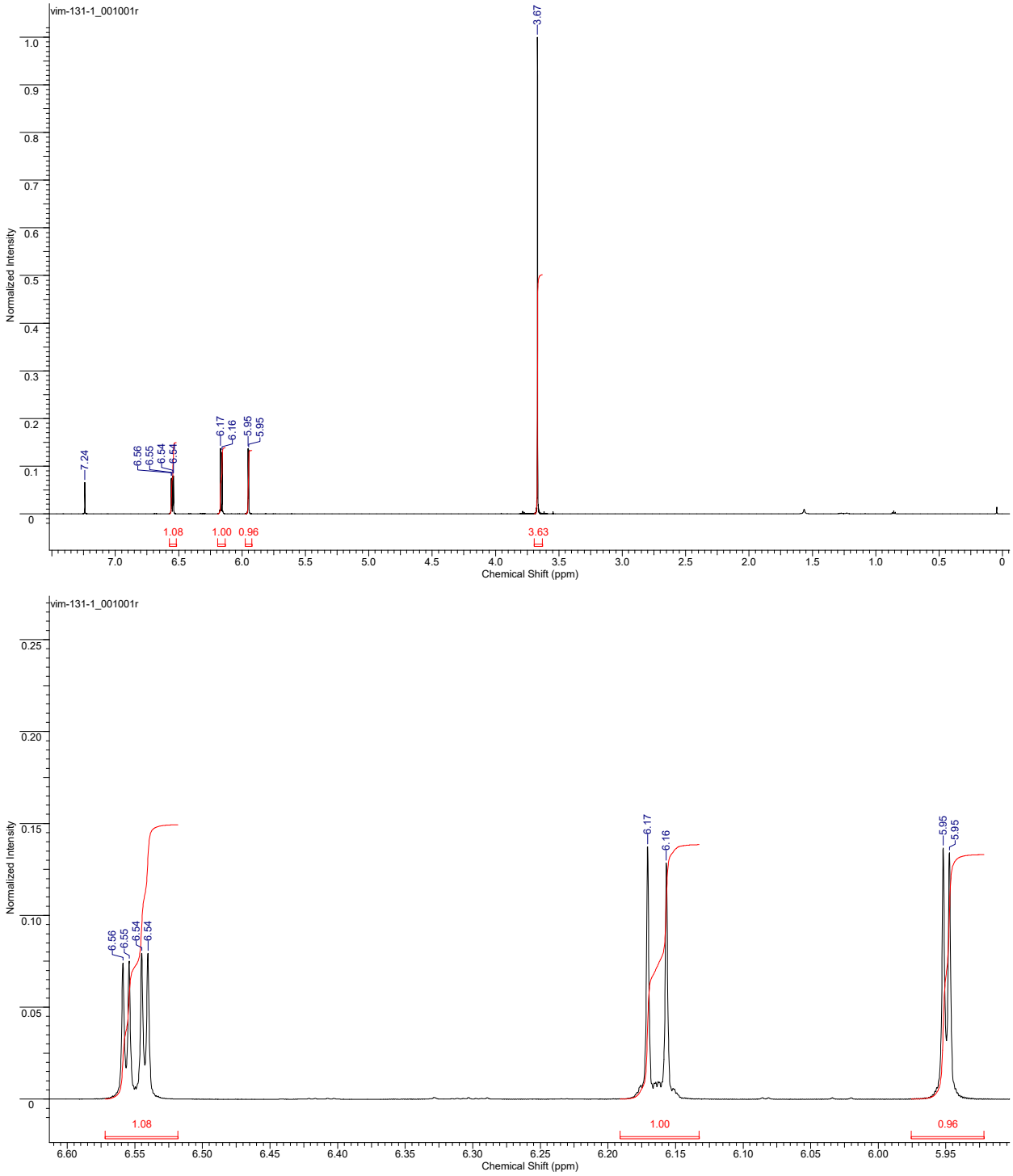

Figure S4 ^{1}H NMR spectrum of compound **3**. Top: the general view. Bottom: downfield part; *J* = 8.2 Hz, 2 Hz.

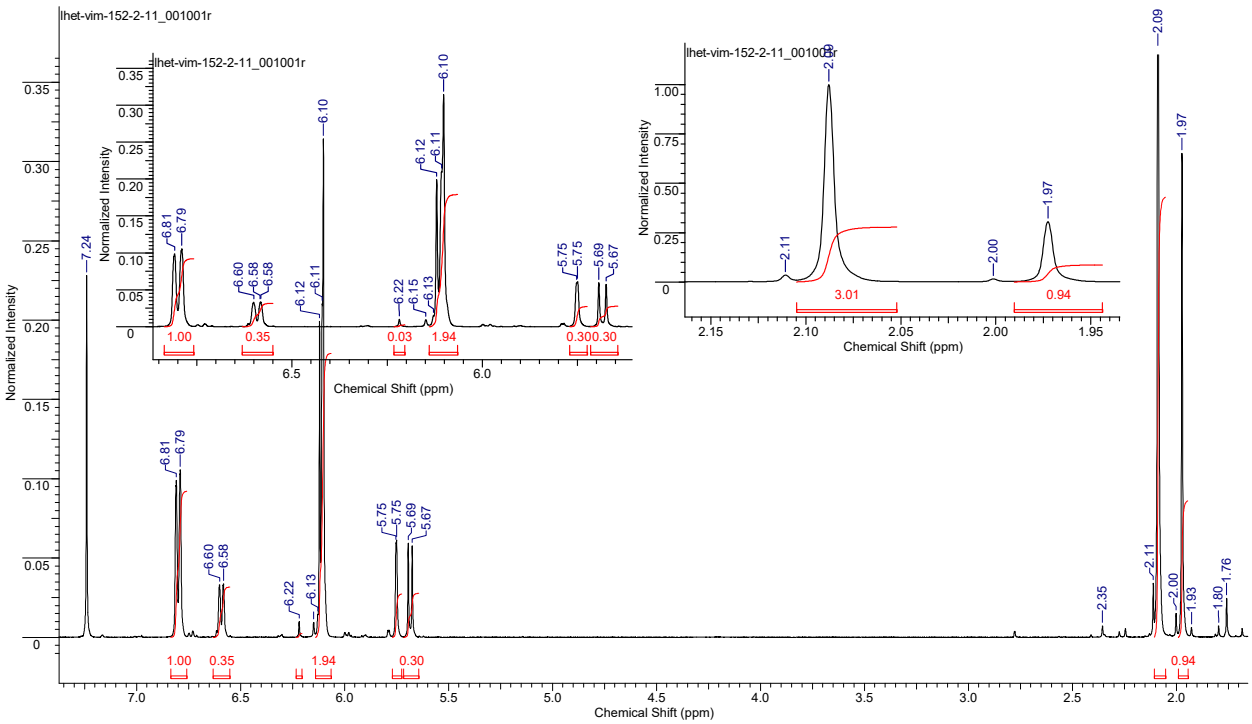

Figure S5 The general view and downfield (left insert) and upfield (right insert) parts of ^{1}H NMR spectrum of the 10:3 mixture of compounds **6** and **8**.

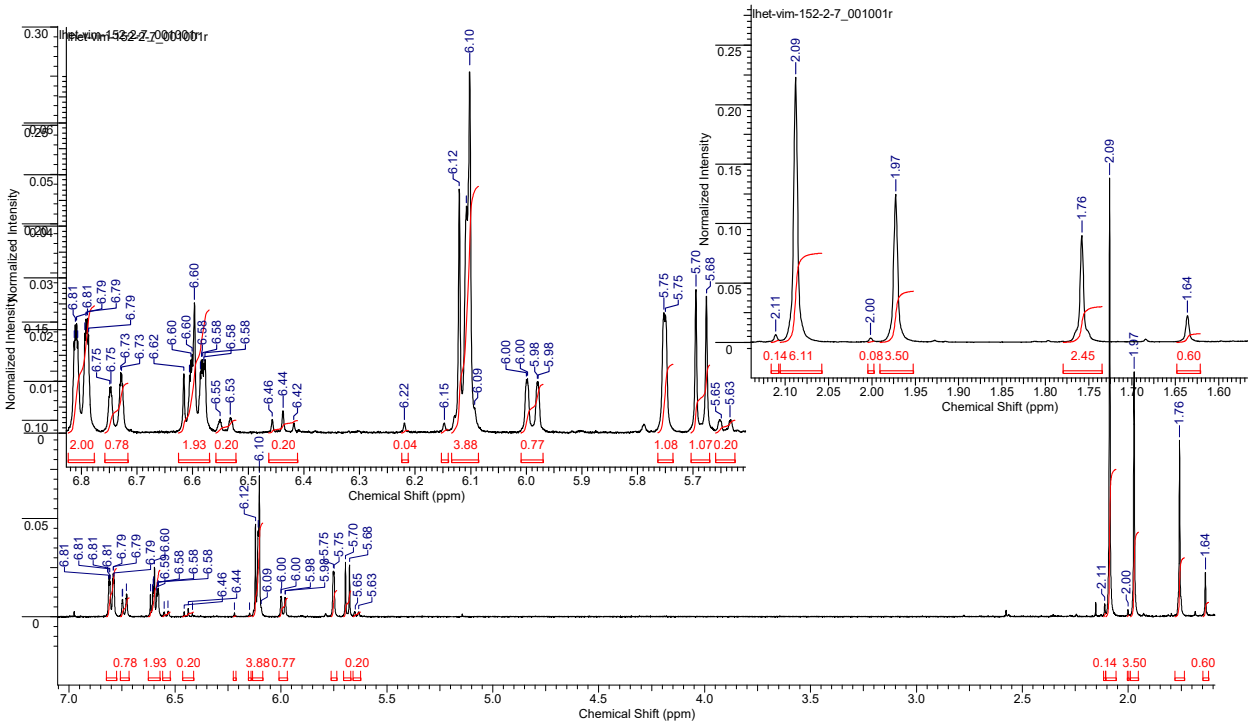

Figure S6 The general view and downfield (left insert) and upfield (right insert) parts of ^{1}H NMR spectrum of a mixture of compounds **5-9**.

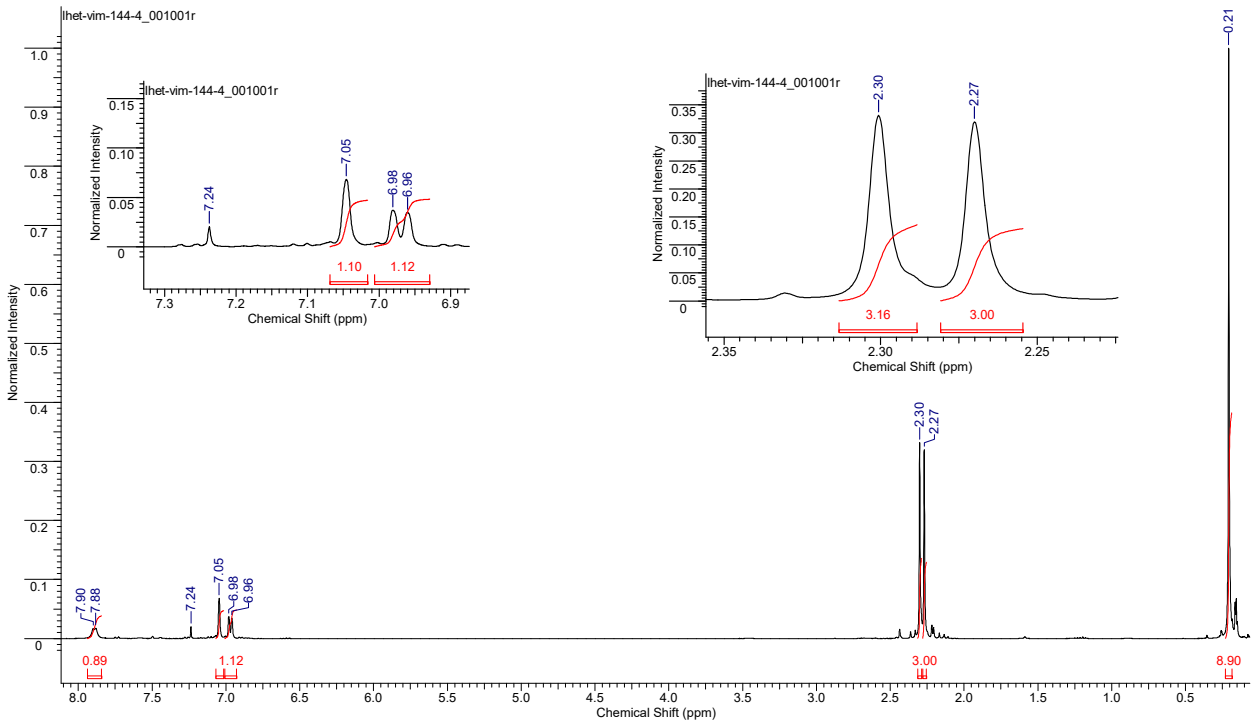

Figure S7 The general view and downfield (left insert) and upfield (right insert) parts of ^{1}H NMR spectrum of compound **10**.

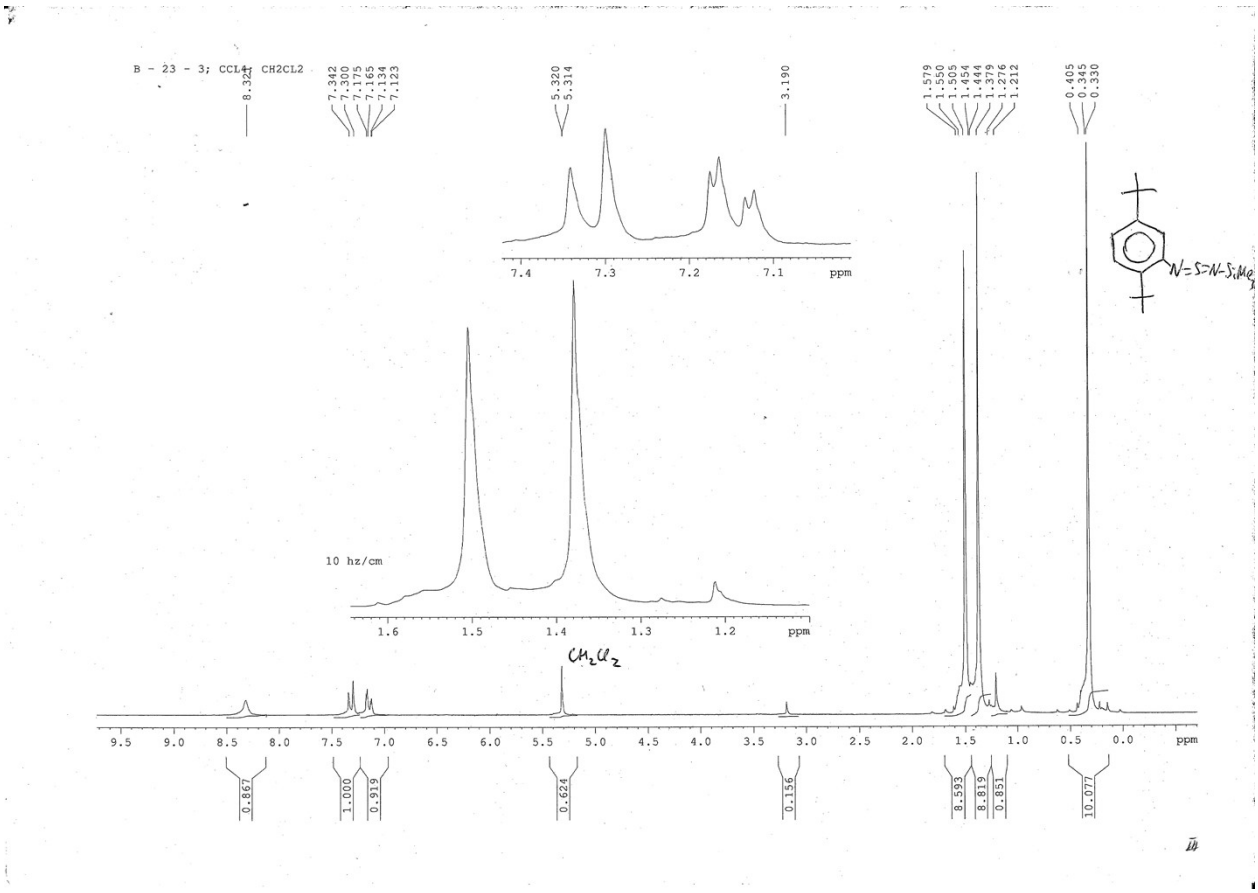

Figure S8 The general view and downfield (upper insert) and upfield (lower insert) parts of ^{1}H NMR spectrum of compound **11**.

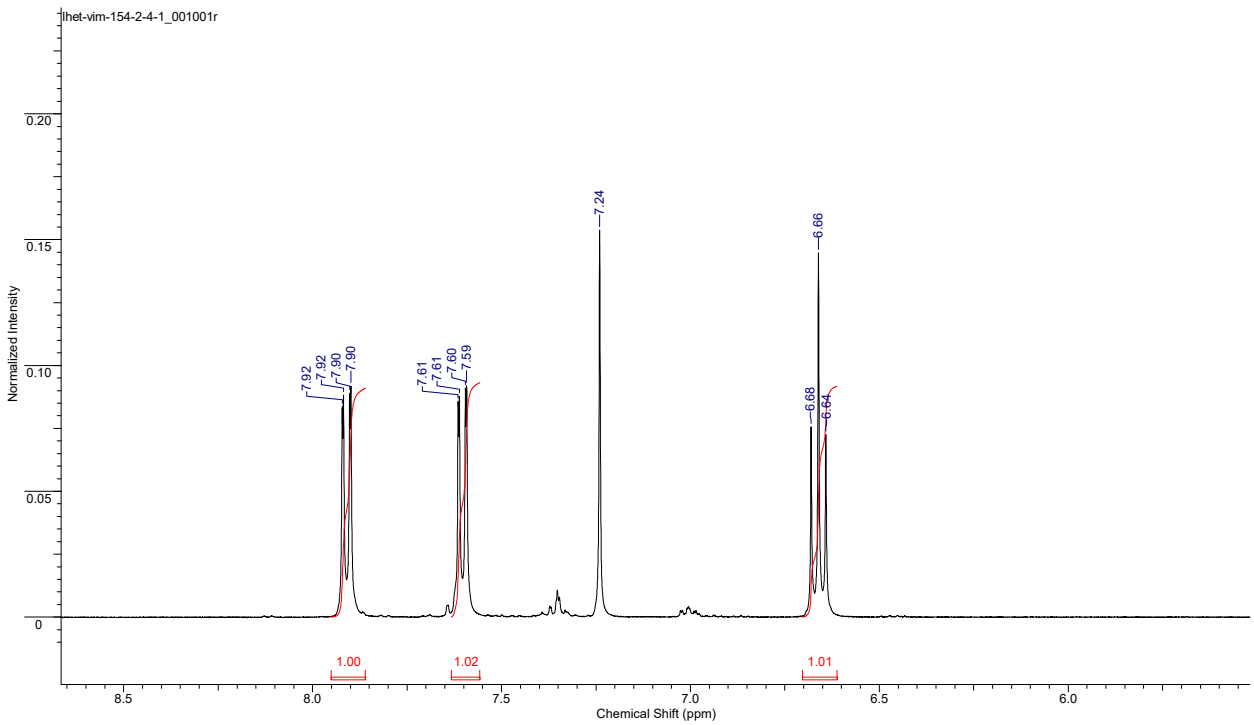

Figure S9 The general view of ^{1}H NMR spectrum of compound **14**.

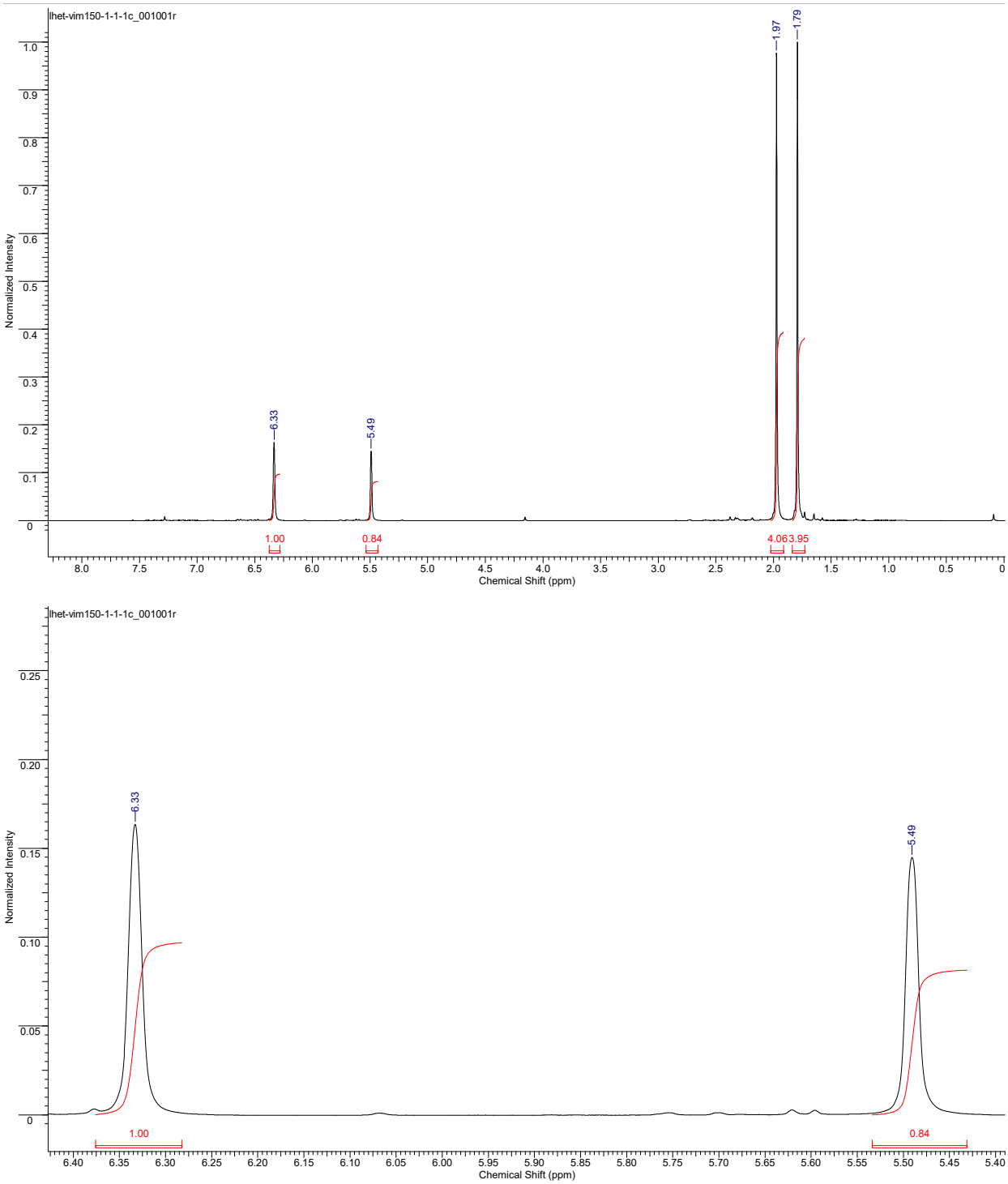

Figure S10 ^{1}H NMR spectrum of compound **15**. Top: the general view. Bottom: downfield part; spin-spin coupling constants *J* are unresolved.

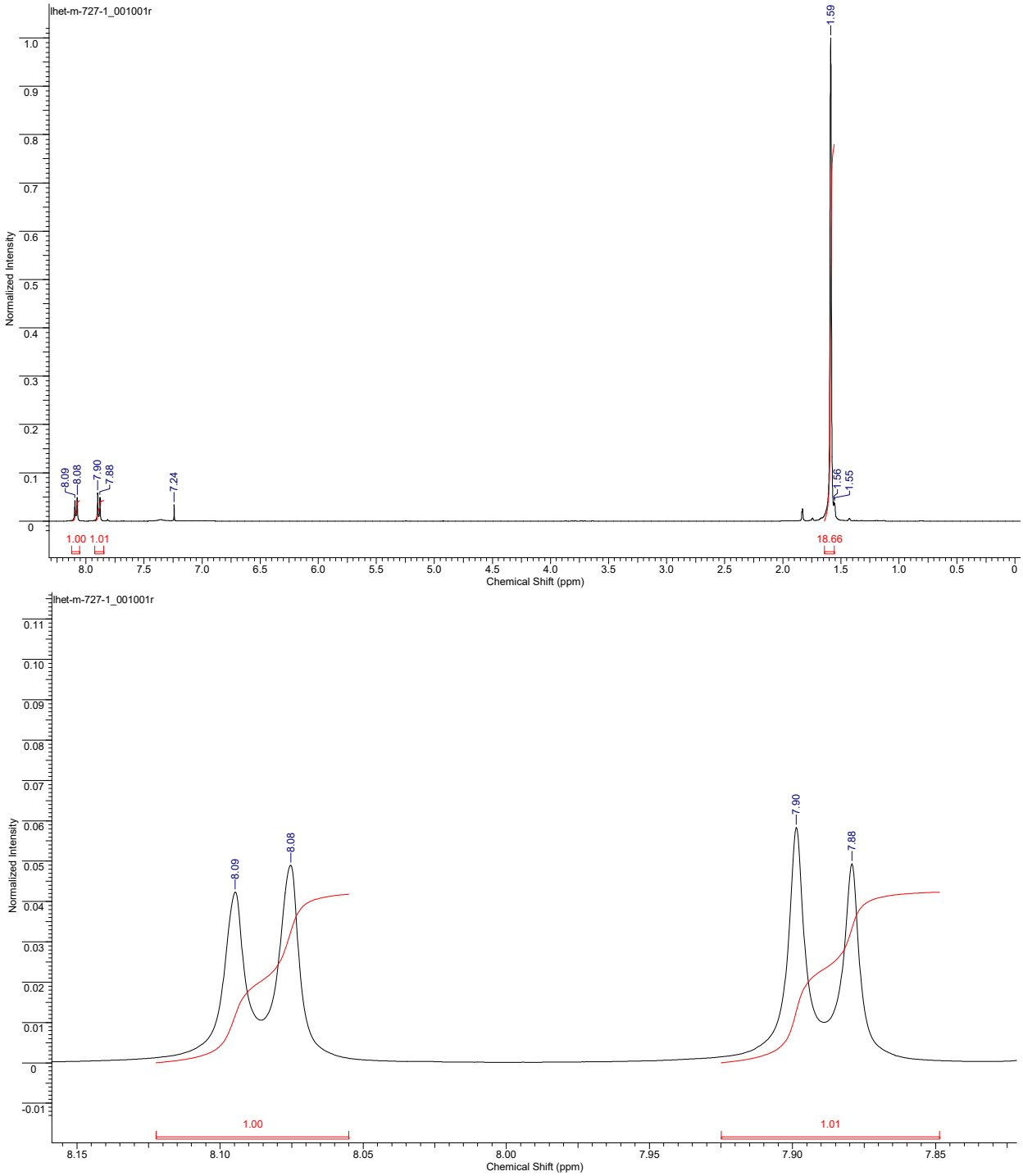

Figure S11 ^{1}H NMR spectrum of compound **25**. Top: the general view. Bottom: downfield part; J = 7.8 Hz.

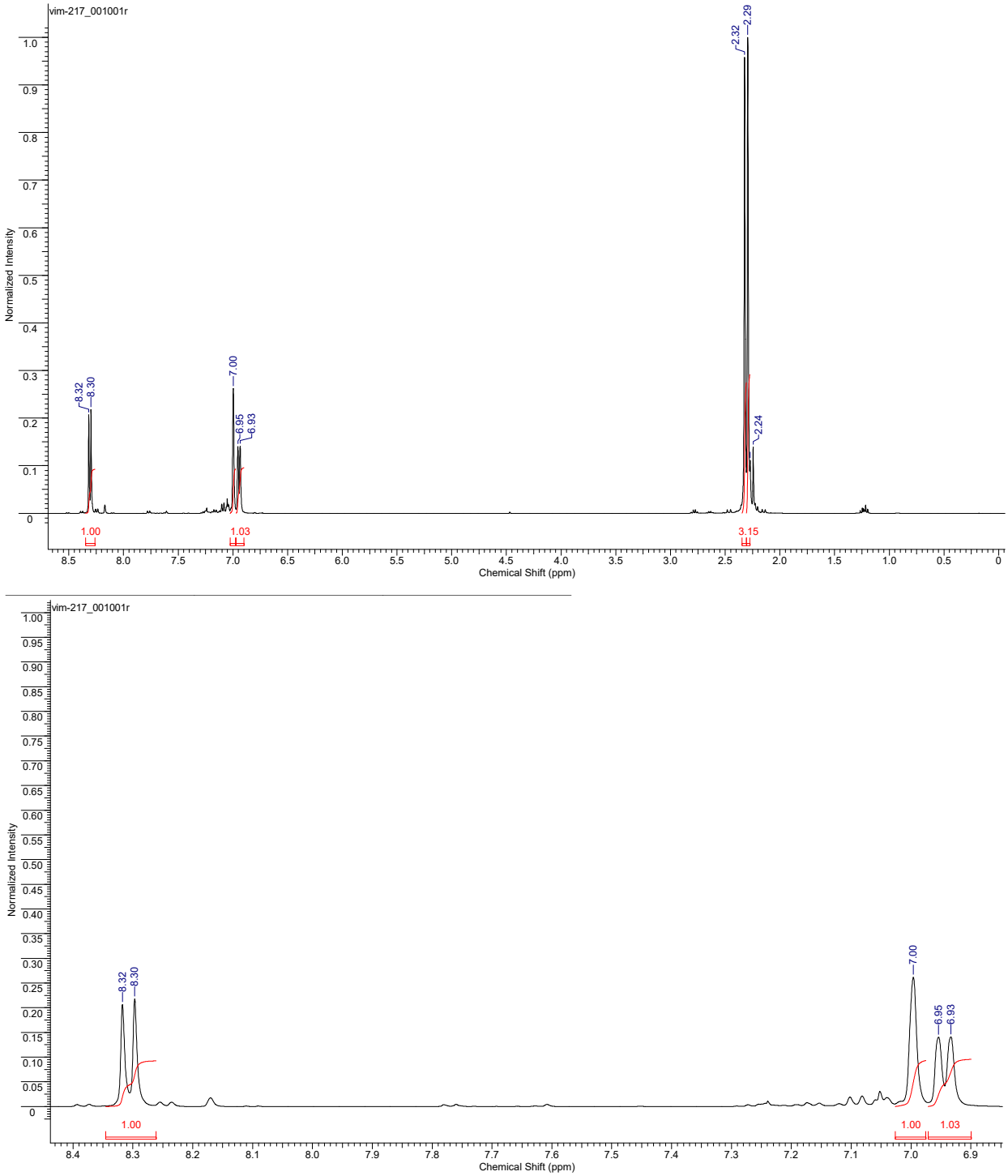

Figure S12 ^{1}H NMR spectrum of compound **34**. Top: the general view. Bottom: downfield part; J = 8.2 Hz.

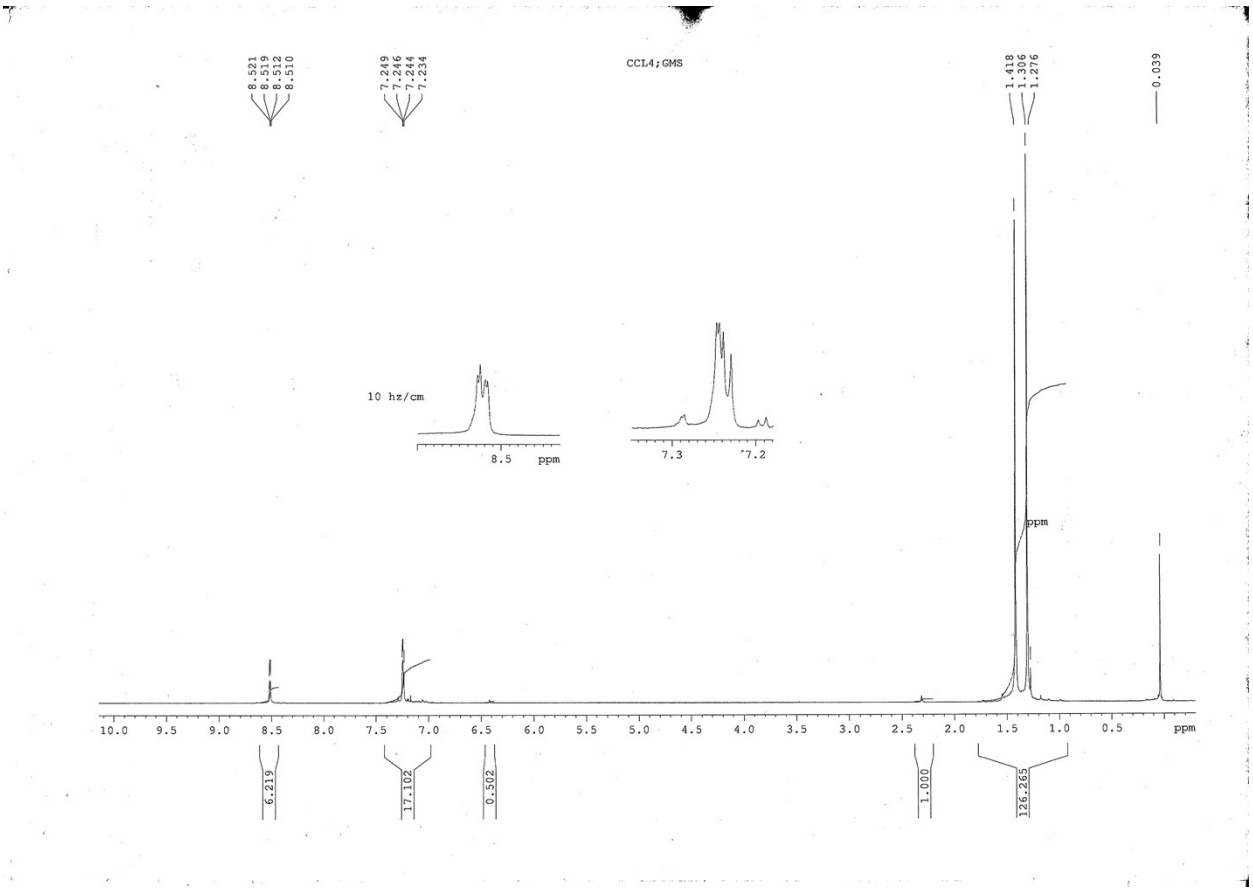

Figure S13 ^{1}H NMR spectrum of compound **35**. The general view and downfield part (inserts). The signal at 7.29-7.19 ppm reveals ABX system with J_{AB} = 8 Hz and δ = 7.24 and 7.25 ppm; other J = 1.9±0.2 Hz and 0.5±0.2 Hz.

^{13}C NMR spectra

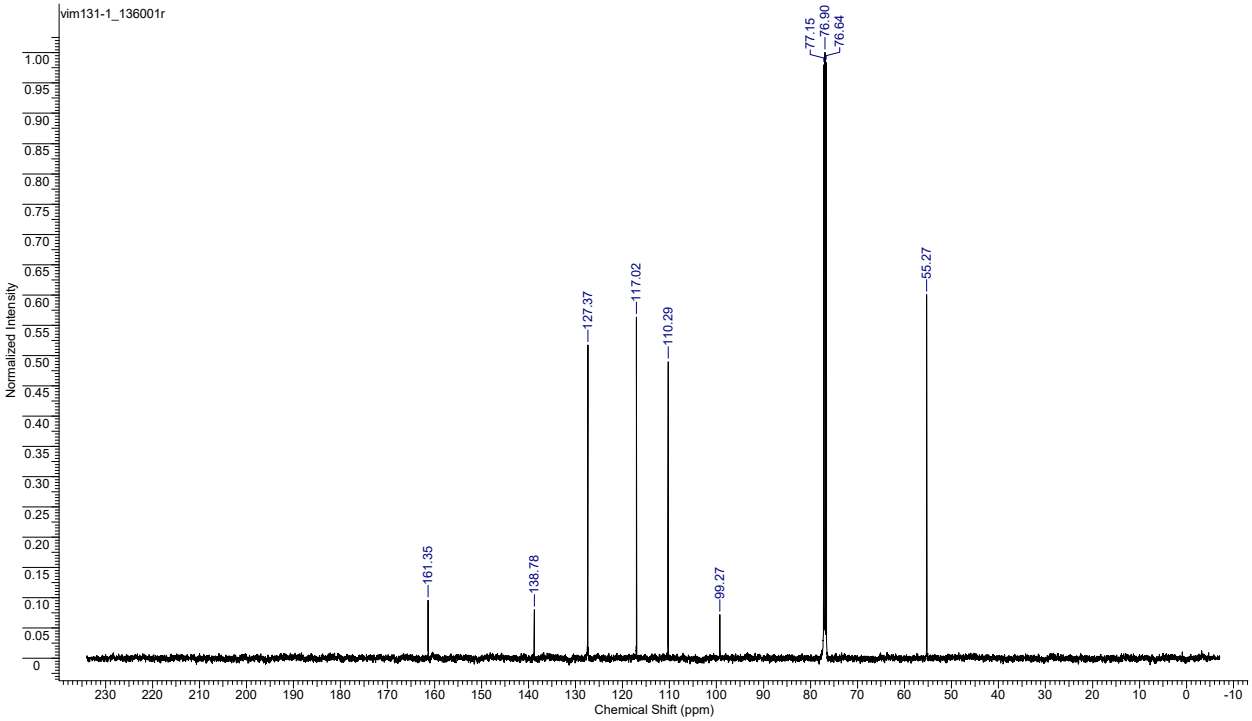

Figure S14 The general view of ^{13}C NMR spectrum of compound **3**.

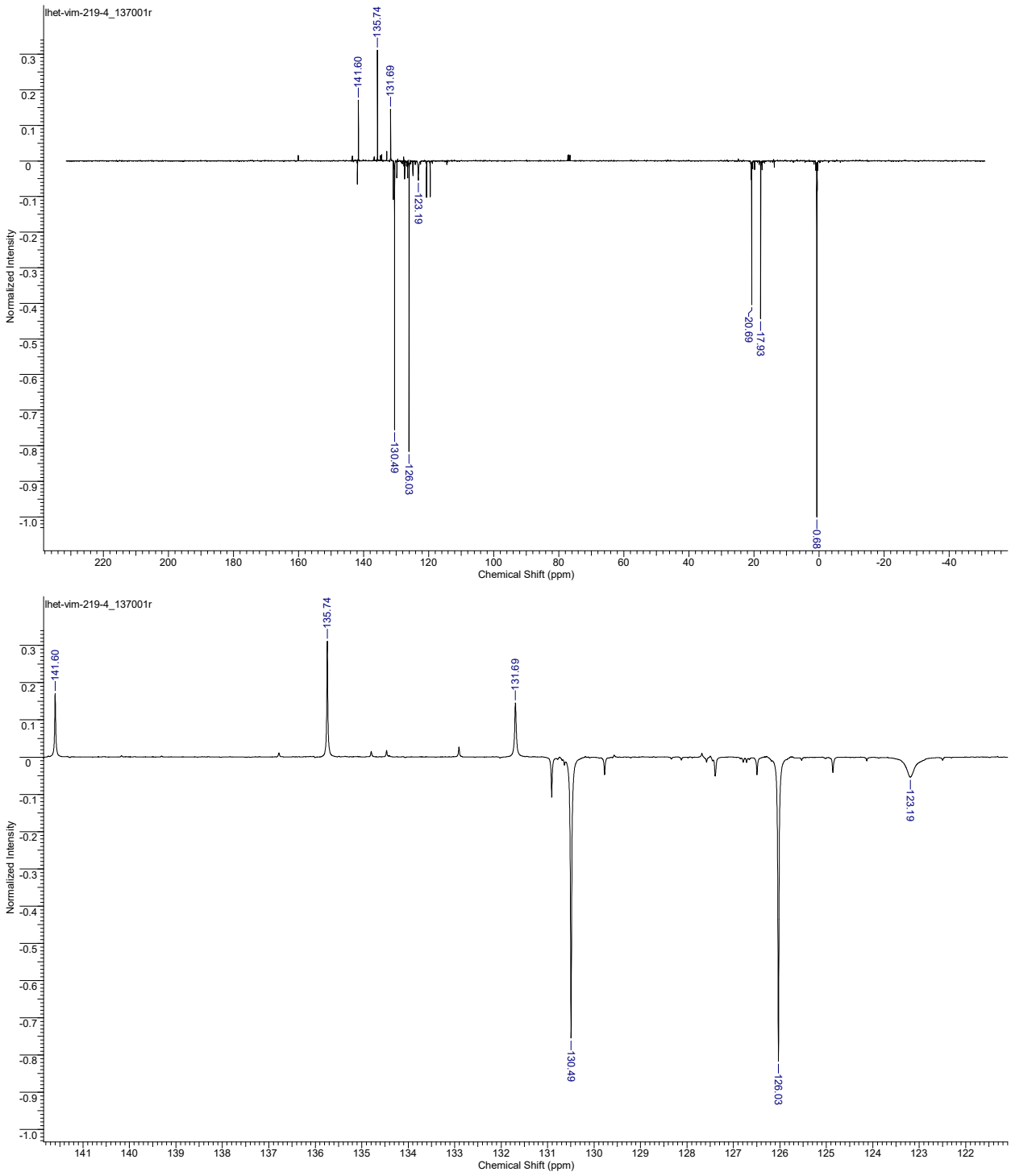

Figure S15 ^{13}C NMR (*J*mod) spectrum of compound **10**. Top: the general view. Bottom: downfield part.

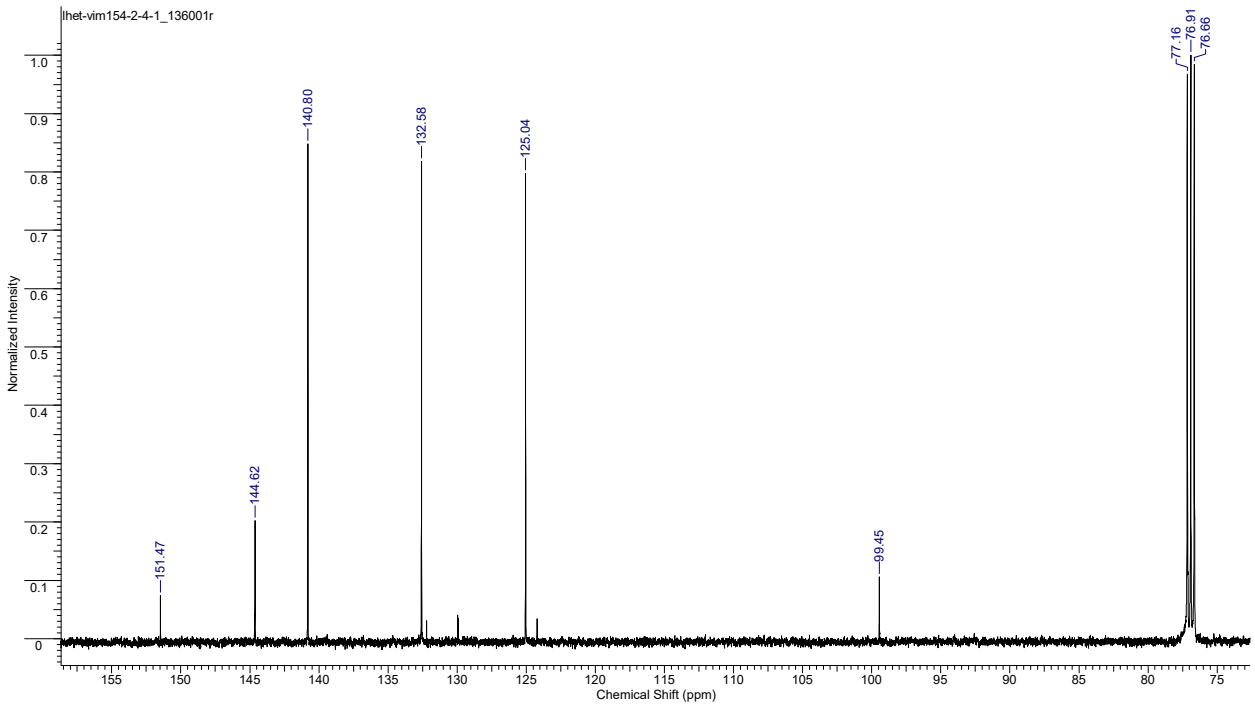

Figure S16 The general view of ^{13}C NMR spectrum of compound **14**.

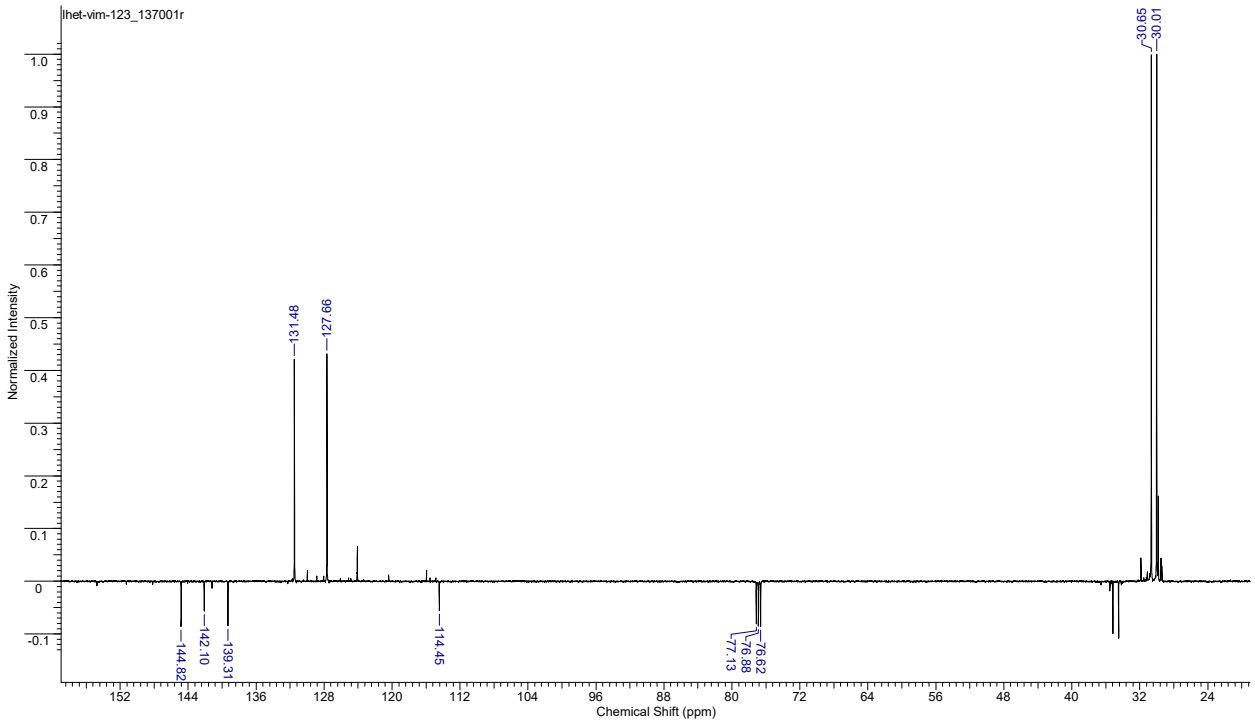

Figure S17 The general view of ^{13}C NMR (*J*mod) spectrum of compound **16**.

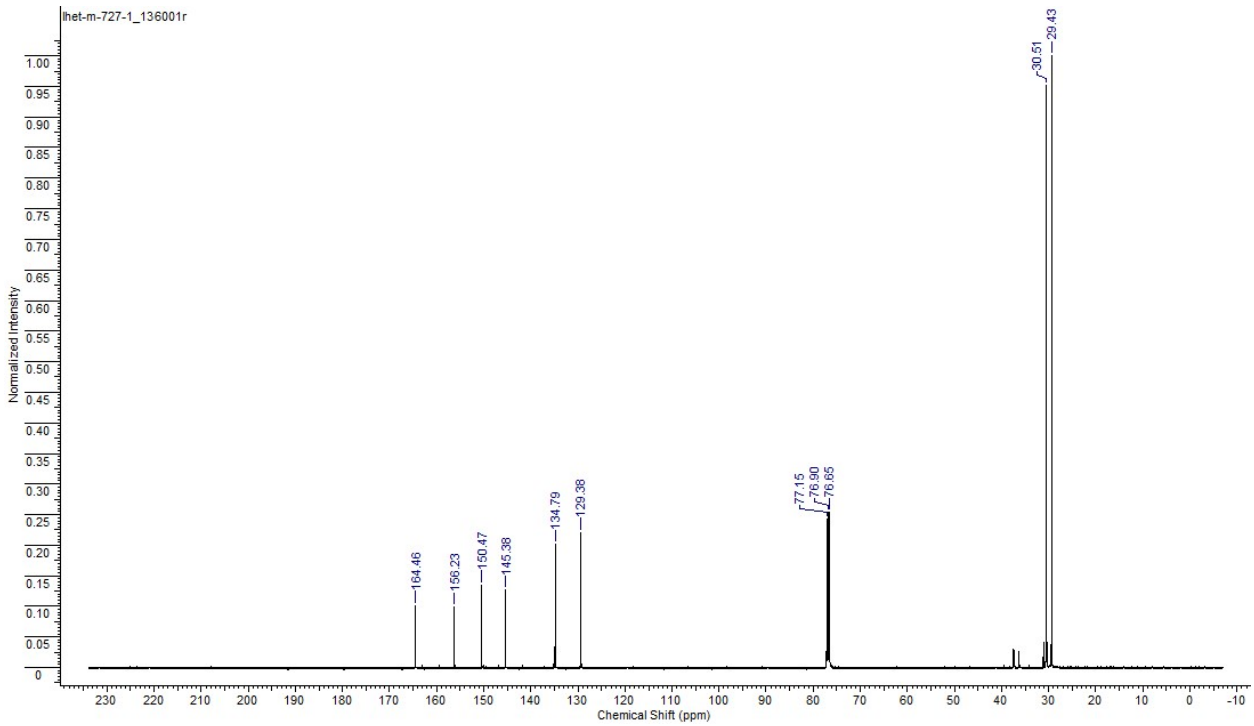

Figure S18 The general view of ^{13}C NMR spectrum of compound **25**.

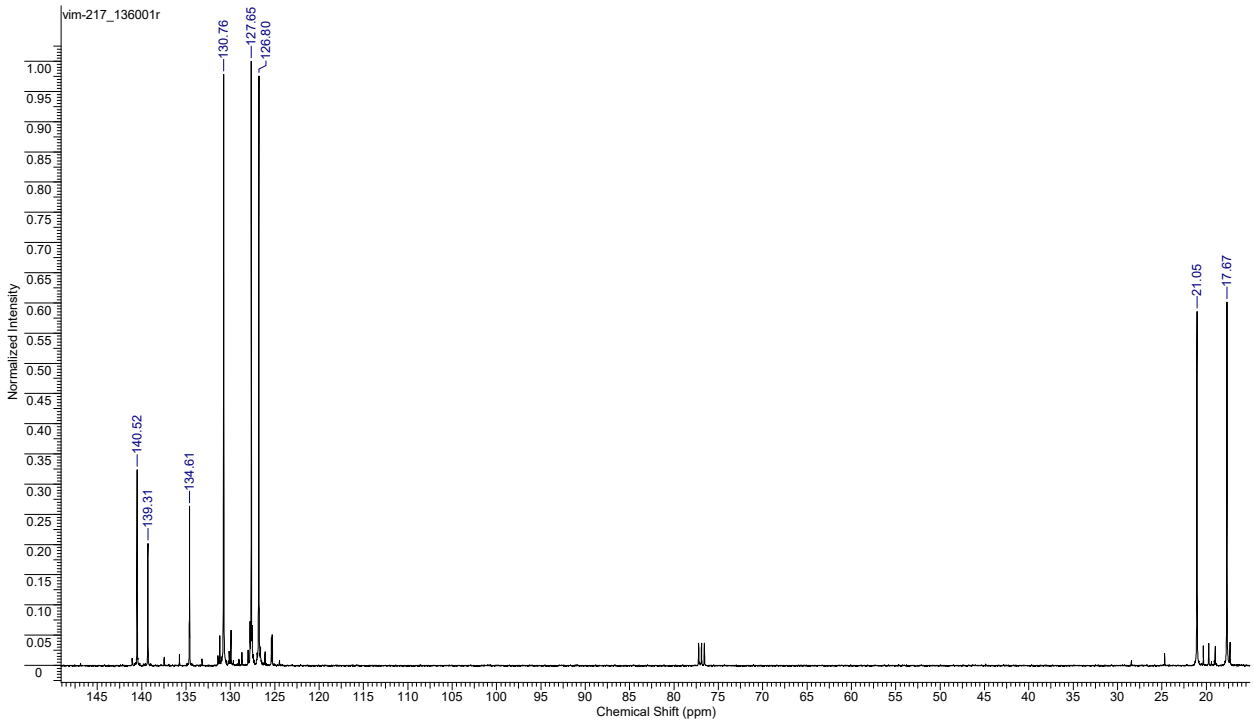

Figure S19 The general view of ^{13}C NMR spectrum of compound **34**.

^{14}N and ^{15}N NMR spectra

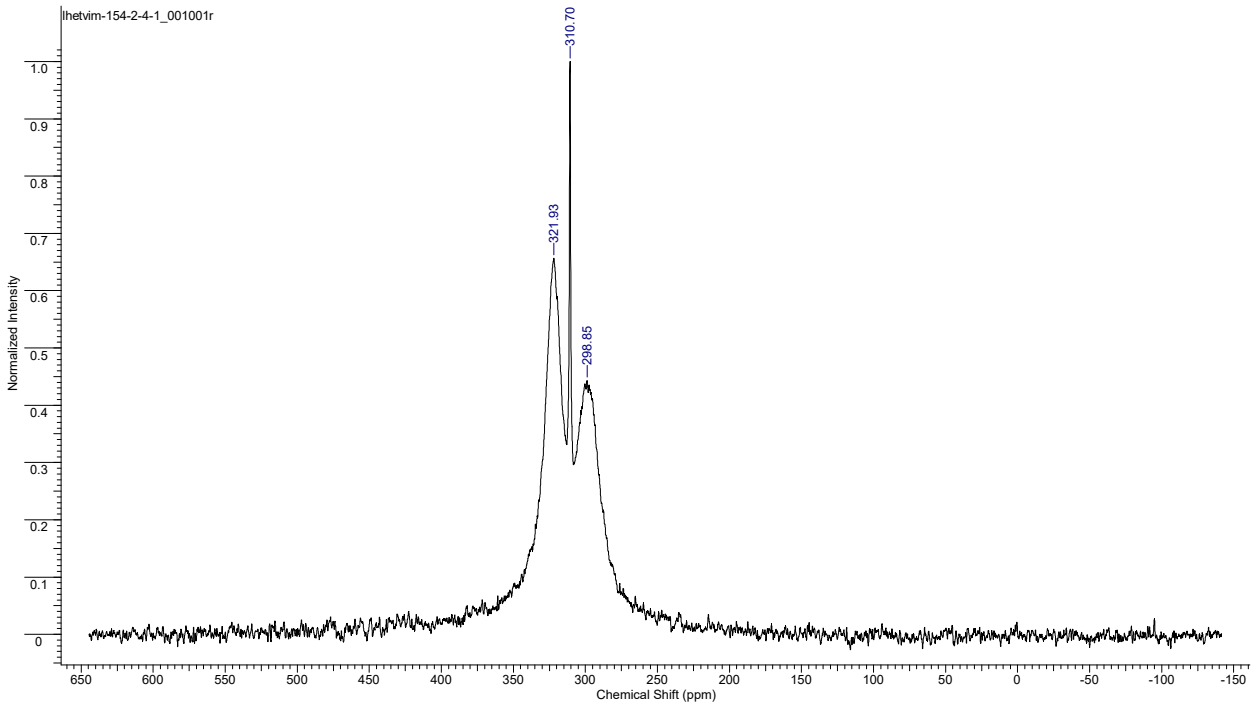

Figure S20 The general view of ^{14}N NMR spectrum of compound **14**.

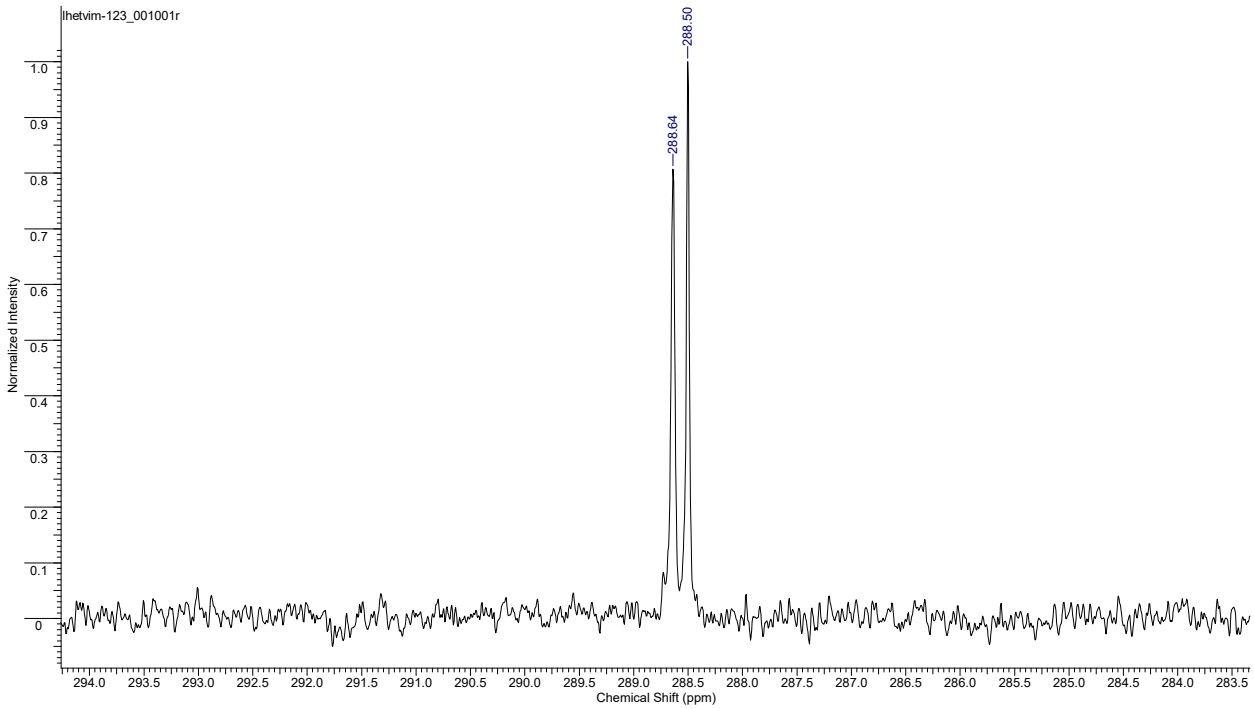

Figure S21 The general view of ^{15}N NMR spectrum of compound **16**.

^{77}Se NMR spectra

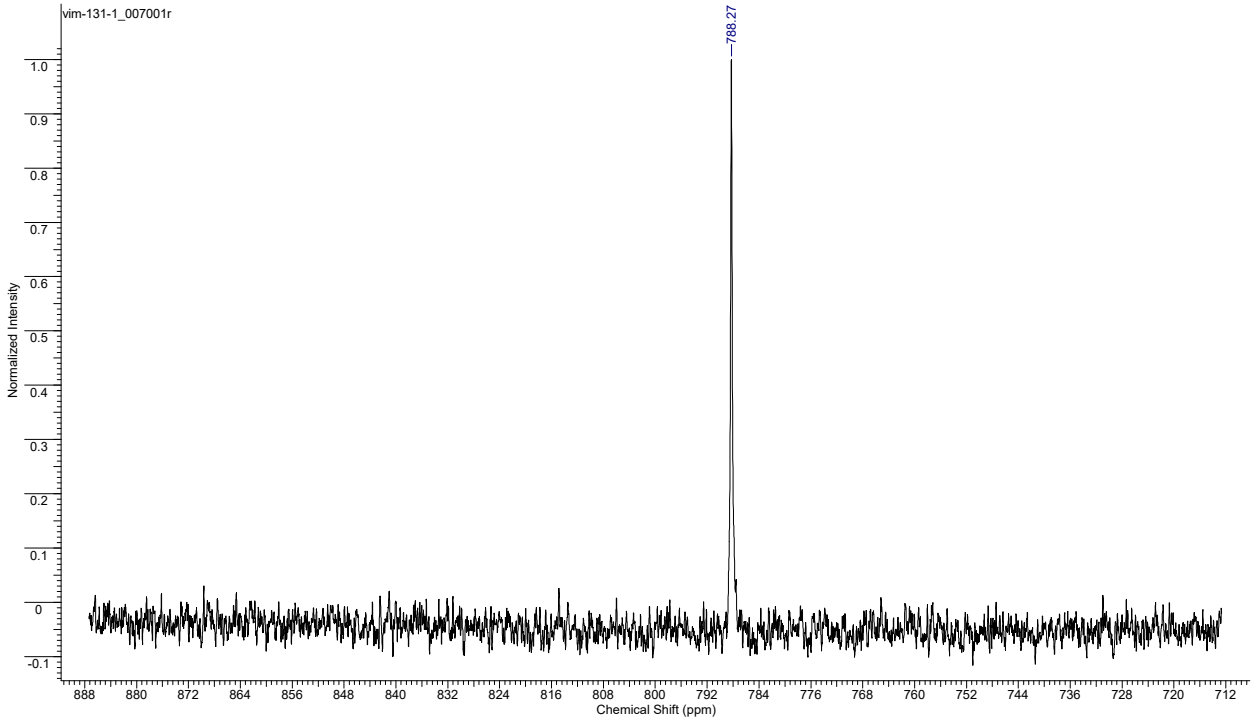

Figure S22 The general view of ^{77}Se NMR spectrum of compound **3**.

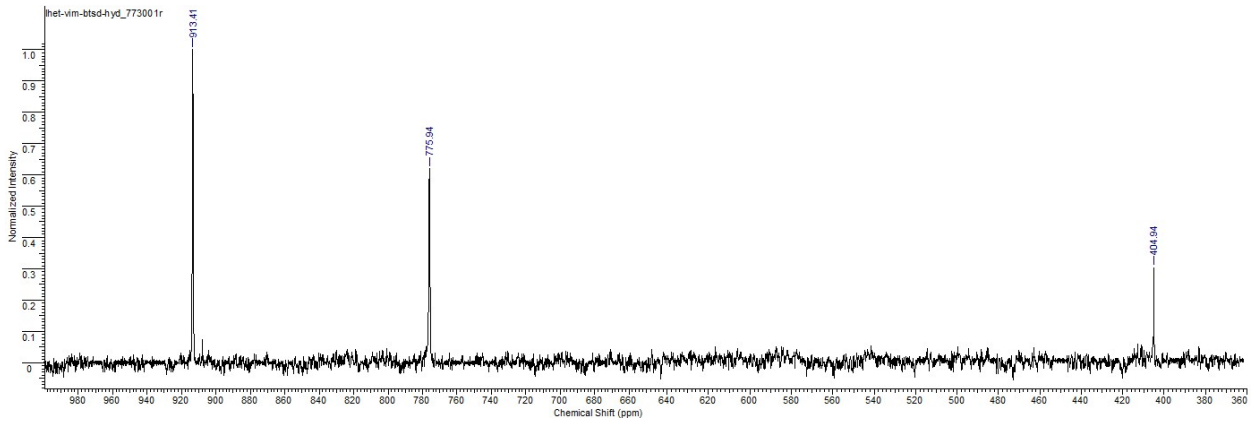

Figure S23 The general view of ^{77}Se NMR spectrum of the mixture of compounds **1**, **29** and 2,2'-diaminodiphenyl diselenide.

4. Thermogravimetry and differential scanning calorimetry

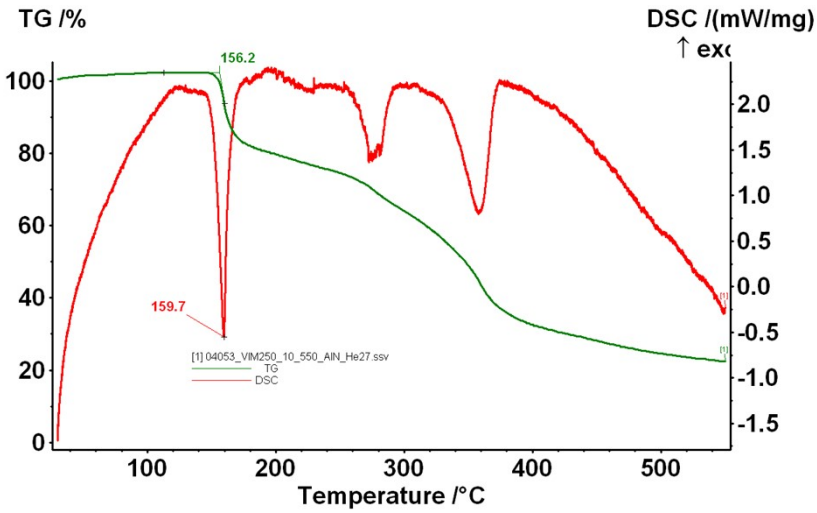

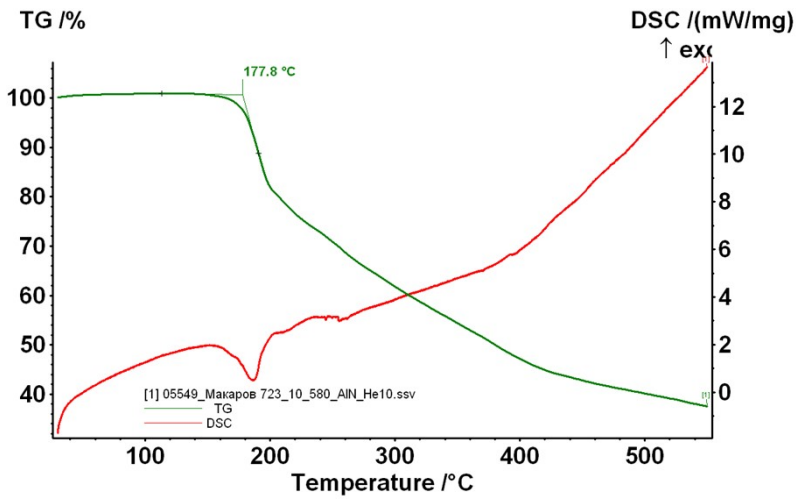

Figure S24 TG / DSC data for salts **27** (top) and **30** (bottom).

5. Electrospray ionization mass spectrometry

ESI-MS data for the products of reaction between 5,8-di-tert-butyl-1,3,2,4-benzodithiadiazine ***16*** *and* SCl_2:

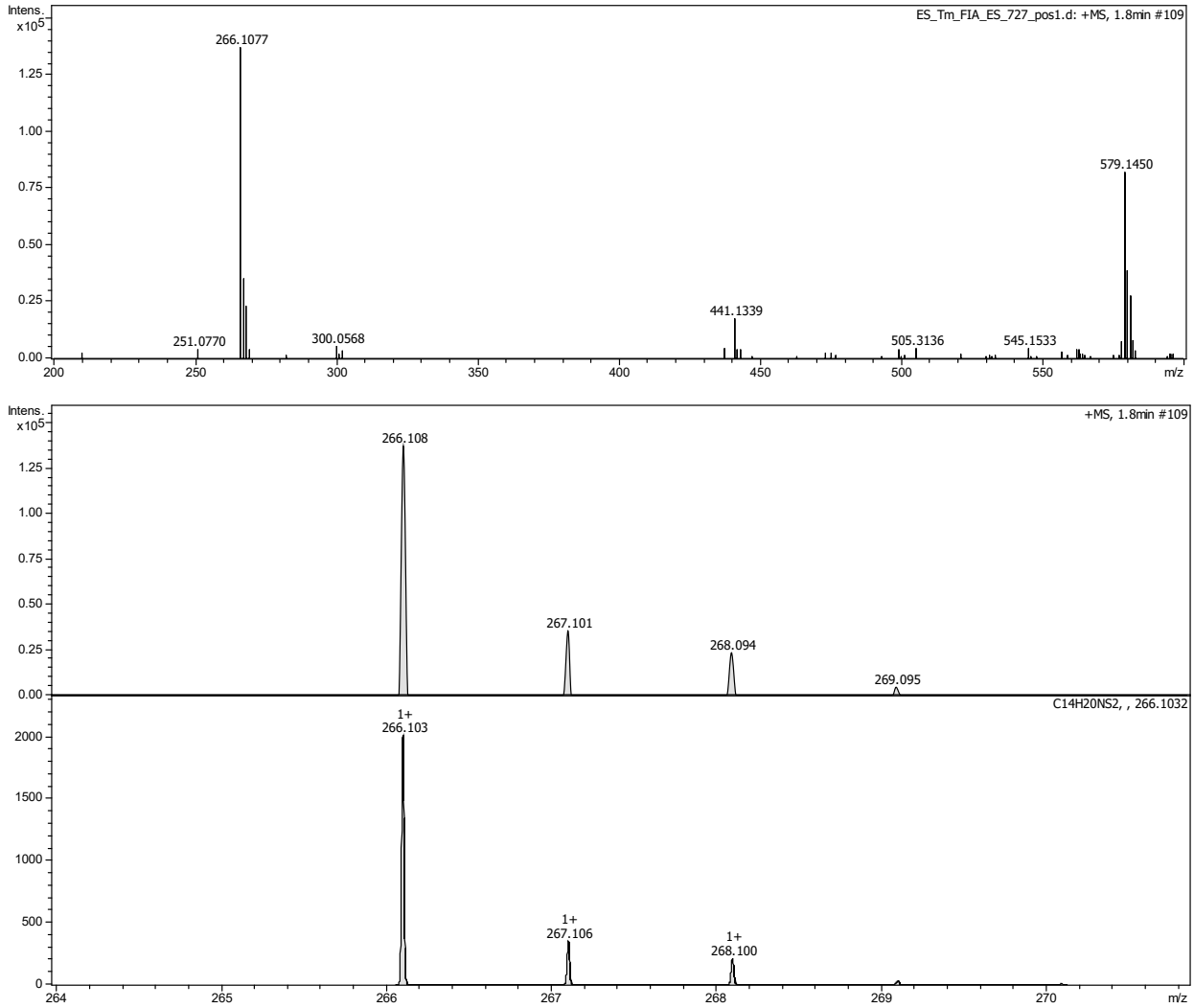

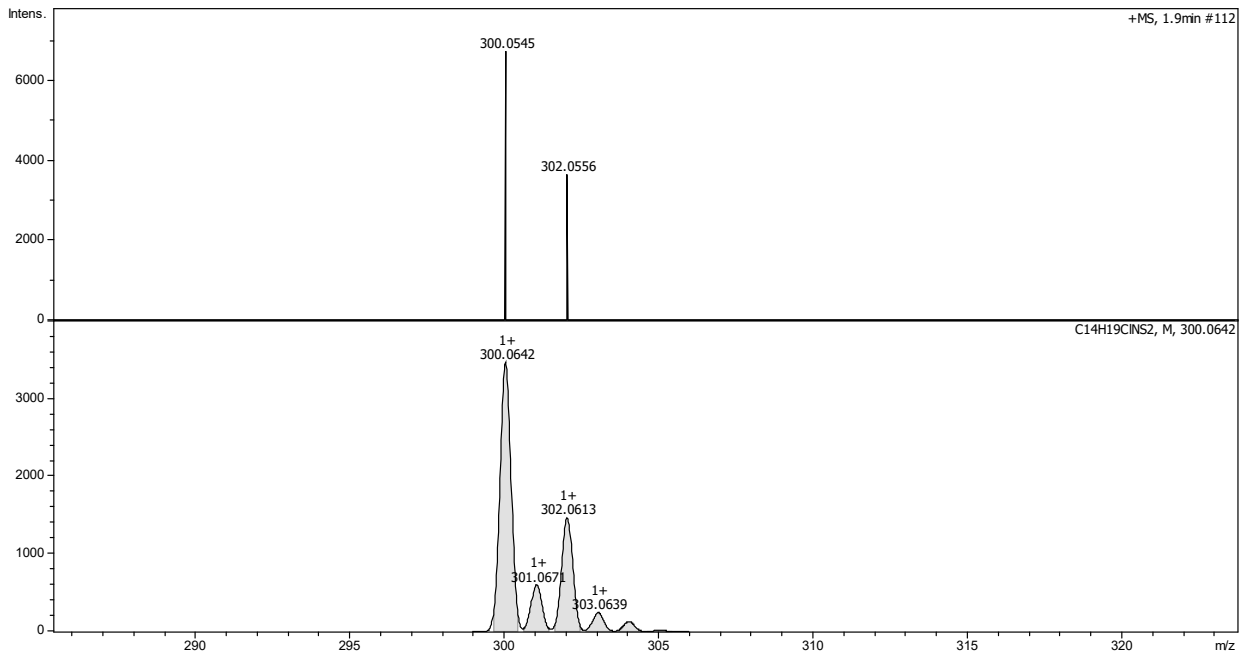

Figure S25 ESI-MS, positive-ion mode spectrum. Above: experimental spectrum featuring the presence of peak with m/z = 266 and the absence of peaks around m/z ~348. Middle: experimental isotopic pattern of the peak with m/z = 266 and its simulation for $C_{14}H_{20}NS_2^+$. Bottom: experimental isotopic pattern of the peak with m/z = 300 (due to low intensity, only 2 main lines are observed) and its simulation for $C_{14}H_{19}ClNS_2^+$.

(*a*)

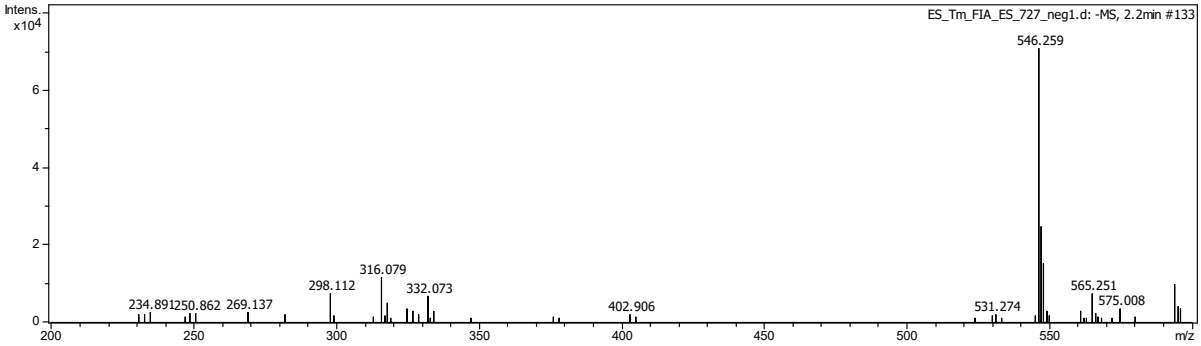
Intens.
x10^4
ES_Tm_FIA_ES_727_neg1.d: -MS, 2.2min #133
546.259
316.079
298.112
332.073
234.891
250.862
269.137
402.906
531.274
565.251
575.008
m/z

(*b*)

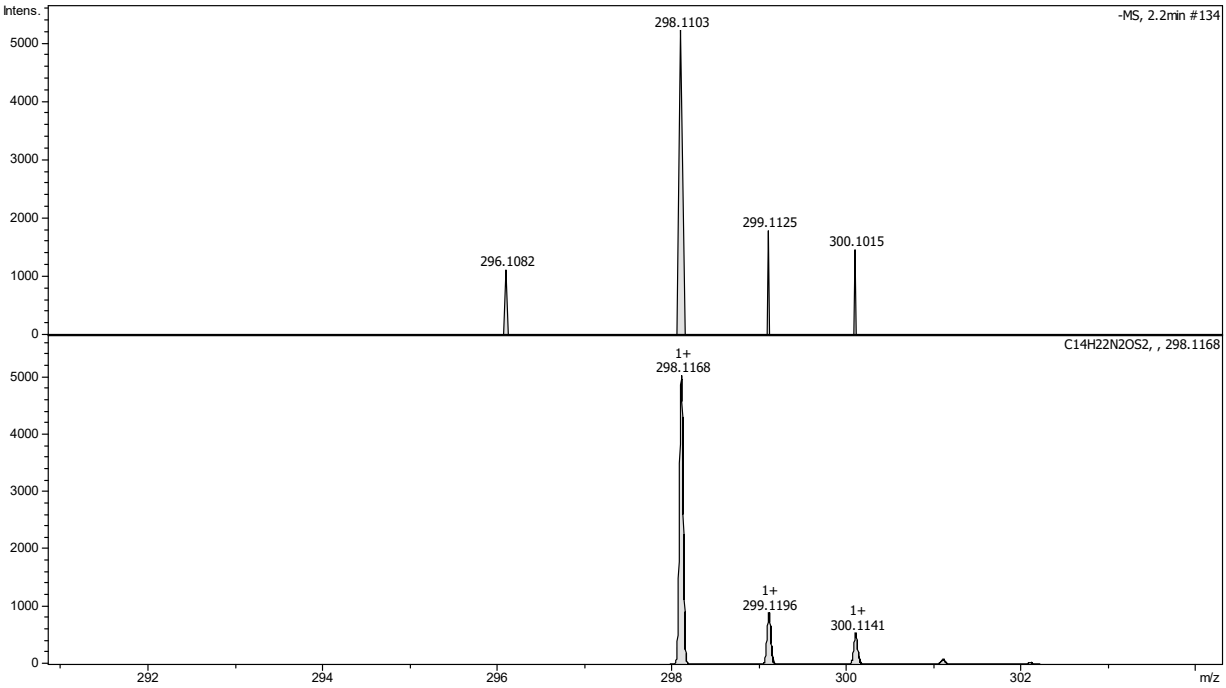
Intens.
-MS, 2.2min #134
298.1103
299.1125
300.1015
296.1082
C14H22N2OS2, , 298.1168
1+
298.1168
1+
299.1196
1+
300.1141
m/z

(*c*)

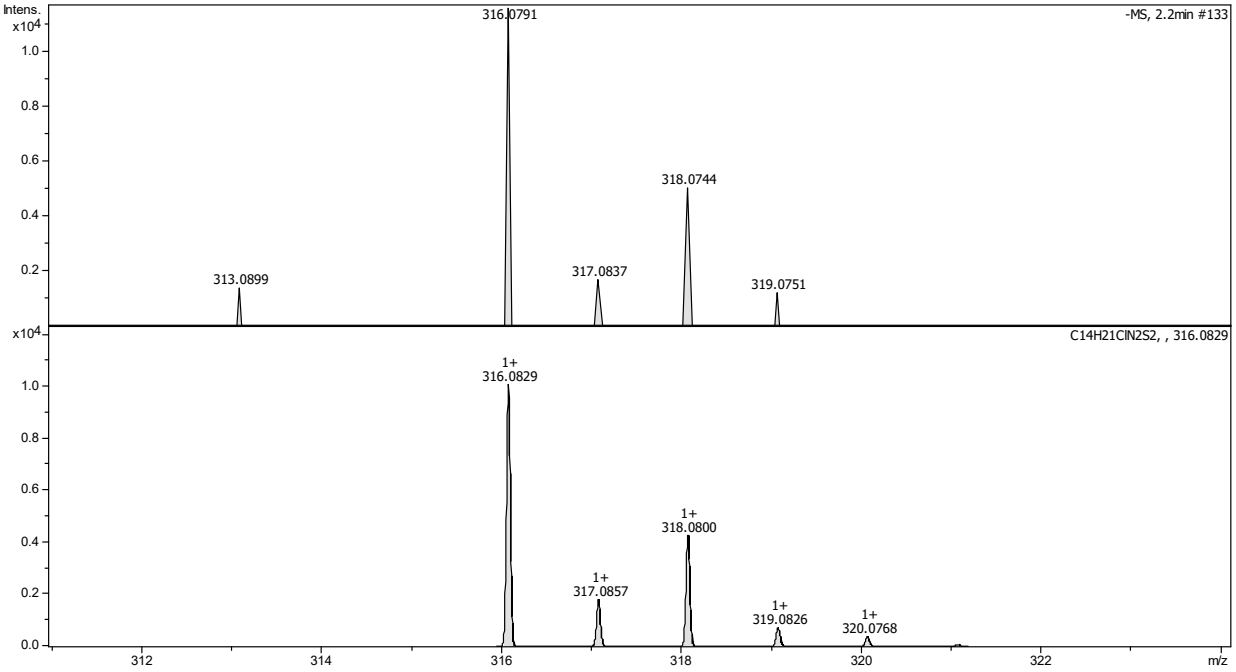
Intens.
x10^4
-MS, 2.2min #133
316.0791
318.0744
313.0899
317.0837
319.0751
C14H21ClN2S2, , 316.0829
1+
316.0829
1+
318.0800
1+
317.0857
1+
319.0826
1+
320.0768
m/z

(*d*)

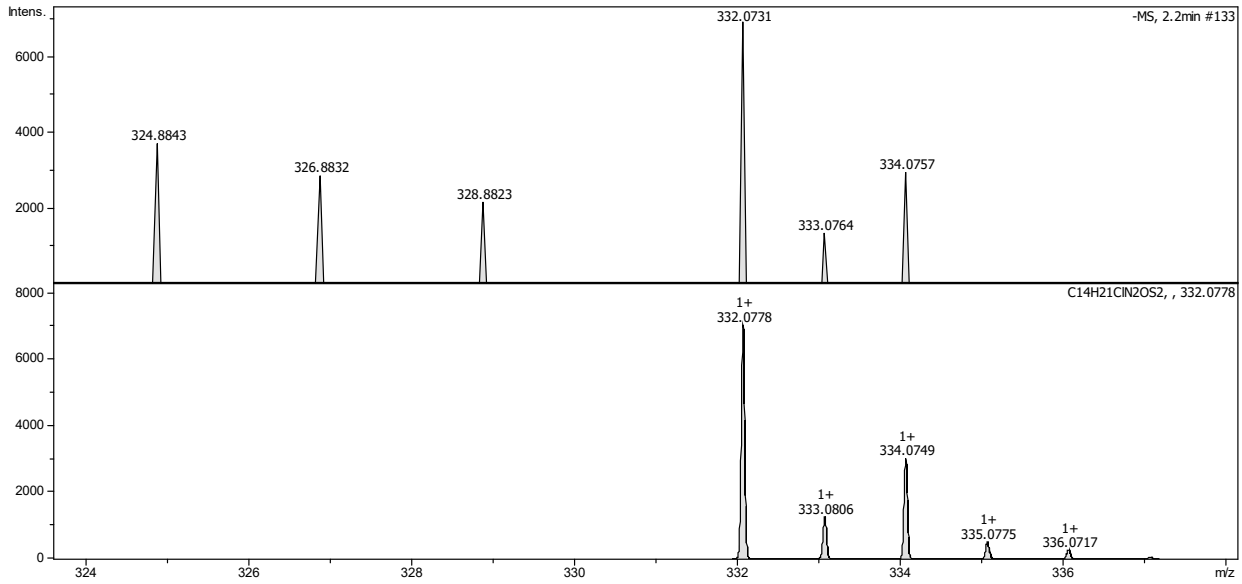

Figure S26 ESI-MS, negative-ion mode spectrum: (*a*) general view of the spectrum; (*b*) experimental isotopic pattern of the peak with m/z = 298 and its simulation for $C_{14}H_{22}N_2OS_2^-$; (*c*) experimental isotopic pattern of the peak with m/z = 316 and its simulation for $C_{14}H_{21}ClN_2S_2^-$; (*d*) experimental isotopic pattern of the peak with m/z = 332 and its simulation for $C_{14}H_{21}ClN_2OS_2^-$.

Table S2 Assignment of ESI-MS data

Spectral mode	M/z	Assignment	Exact mass	Relative error, ppm
Positive ions	266.108	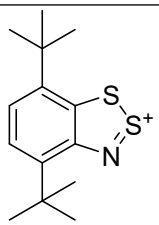	266.103 ($C_{14}H_{20}NS_2^+$)	19
	300.055	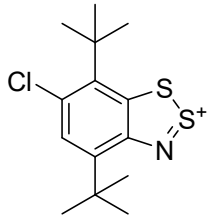	300.064 ($C_{14}H_{19}ClN_2S^+$)	32
Negative ions	282.114	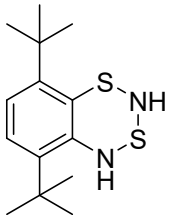	282.122 ($C_{14}H_{22}N_2S_2^-$); isotopic pattern was not analysed due to low intensity	27
	298.117	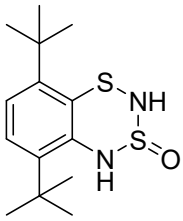	298.110 ($C_{14}H_{22}N_2OS_2^-$)	22
	316.079	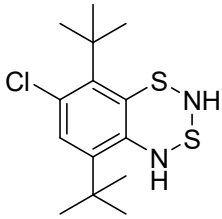	316.083 ($C_{14}H_{21}ClN_2S_2^-$)	12
	332.073	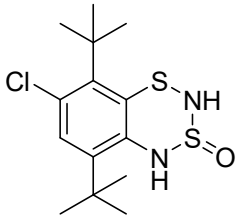	332.079 ($C_{14}H_{21}ClN_2OS_2^-$)	14

6 References

1 (*a*) M. Mantina, A. C. Chamberlin, R. Valero, C. C. Cramer and D. J. Truhlar, *J. Chem. Soc. A,* 2009, **113**, 5806–5812; (*b*) R. S. Rowland and R. Taylor, *J. Phys. Chem.,* 1996, **100**, 7384–7391; (*c*) A. Bondi, *J. Phys. Chem.*, 1964, **68**, 441–451.

2 *(a)* A. Yu. Makarov, I. Yu. Bagryanskaya, Yu. V. Gatilov, T. V. Mikhalina, M. M. Shakirov, L. N. Shchegoleva and A. V. Zibarev, *Heteroatom Chem.,* 2001, **12**, 563–576; *(b)* I. Yu. Bagryanskaya, Yu. V. Gatilov, A. Yu. Makarov, A. M. Maksimov, A. O. Miller, M. M. Shakirov and A. V. Zibarev, *Heteroatom Chem.,* 1999, **10**, 113–124; *(c)* A. V. Zibarev, A. O. Miller, Yu. V. Gatilov and G. G. Furin, *Heteroatom Chem.*, 1990, **1**, 443–453.

3 A. R. Katritzky, B. V. Rogovoy, C. Chassaing, V. Vvedensky, B. Forood, B. Flatt and H. Nakai, *J. Het. Chem.*, 2000, **37**, 1655–1658.